The Mitochondrial Copper Metallochaperone Cox17 Exists as an Oligomeric, Polycopper Complex†

Daren N. Heaton,‡ Graham N. George,§ Garth Garrison,‡ and Dennis R. Winge*,‡

University of Utah Health Sciences Center, 50 North Medical Drive, Salt Lake City, Utah 84132, and Stanford Synchrotron Radiation Laboratory, Stanford University SLAC, P.O. Box 4393, Stanford, California 94309

Received October 3, 2000; Revised Manuscript Received November 15, 2000

ABSTRACT: Cox17 is the candidate copper metallochaperone for delivery of copper ions to the mitochondrion for assembly of cytochrome *c* oxidase. Cox17 purified as a recombinant molecule lacking any purification tag binds three Cu(I) ions per monomer in a polycopper cluster as shown by X-ray absorption spectroscopy. The CuCox17 complex exists in a dimer/tetramer equilibrium with a 20 μM k_d. The spectroscopic data do not discern whether the dimeric complex forms a single hexanuclear Cu(I) cluster or two separate trinuclear Cu(I) clusters. The Cu(I) cluster(s) exhibit(s) predominantly trigonal Cu(I) coordination. The cluster(s) in Cox17 resemble(s) the polycopper clusters in Ace1 and the Cup1 metallothionein in being pH-stable and luminescent. The physical properties of the CuCox17 complex purified as an untagged molecule differ from those reported previously for a GST−Cox17 fusion protein. The CuCox17 cluster is distinct from the polycopper cluster in Cup1 in being labile to ligand exchange. CuCox17 localized within the intermitochondrial membrane space appears to be predominantly tetrameric, whereas the cytosolic CuCox17 is primarily a dimeric species. Cys→Ser substitutions at Cys23, Cys24, or Cys26 abolish the Cox17 function and prevent tetramerization, although Cu(I) binding is largely unaffected. Thus, the oligomeric state of Cox17 may be important to its physiological function.

The terminal oxidase of respiration is the cytochrome *c* oxidase complex IV found in the inner mitochondrial membrane. Complex IV from bovine heart consists of 13 subunits, 3 of which are encoded by the mitochondrial genome (*1*−*3*). Assembly of the active oxidase complex requires the insertion of four types of cofactors including two heme *a* groups, three copper ions, one Zn(II) ion, and one Mg(II) ion (*2*). Accessory proteins are critical for assembly of the active oxidase (*4*−*7*). Two of these accessory proteins are enzymes required for the modification of protoheme to heme *a* (isoprenylation and formylation). Cox10 appears to function in the isoprenylation of protoheme (*5*). The oxygenase responsible for the formylation modification remains unclear in yeast, although the gene is known in *Bacillus subtilis* (*8*). The delivery and insertion of Cu ions in cytochrome *c* oxidase appear to require at least three proteins: Cox17, Sco1, and Cox11 (*9*−*12*). Two Cu ions are inserted into subunit 2, forming the binuclear Cu_A site, and a single Cu ion into subunit 1, forming the binuclear Cu−heme a_3 reaction center (*2*). Since both subunits 1 and 2 are mitochondrially synthesized, Cu ion insertion must occur within the mitochondrion.

Cox17 appears to be a copper metallochaperone necessary for delivery of copper ions to the mitochondrion. Cells lacking a functional Cox17 molecule are respiratory-deficient, but synthesize both mitochondrial and nuclear-encoded cytochrome oxidase subunits (*9*). The role of Cox17 as a metallochaperone was implicated by the observed suppression of the respiratory defect of *cox17*Δ cells by high exogenous Cu(II) levels (*9*). The effect of exogenous Cu(II) was specific to *cox17* mutant cells (*9*). Two additional observations are consistent with this putative function as a metallochaperone shuttle. First, Cox17 is localized in the cytosol and intermitochondrial membrane space (*13*). Second, Cox17 is a Cu(I) binding protein with at least two Cu(I) ions bound in a polycopper cluster (*13, 14*). Three cysteinyl residues present in a CysCysXaaCys sequence motif are critical for Cox17 function (*15*). Single substitution of any of these three cysteines with serines results in a nonfunctional cytochrome oxidase complex. Cells harboring such a mutation fail to grow on nonfermentable carbon sources and have no cytochrome *c* oxidase activity in isolated mitochondria. Mutant proteins containing a double Cys→Ser mutation in this motif fail to bind Cu(I) (*15*).

Sco1 is an inner mitochondrial membrane protein important specifically in cytochrome oxidase assembly (*16*). Cells lacking a functional Sco1 are defective in cytochrome oxidase activity, and this phenotype is not reversed by the addition of high exogenous copper (*10*). However, the phenotype of *cox17-1* cells harboring a Cys→Tyr substitution in Cox17 was suppressed by high-copy *SCO1* or the

† This work was supported by Grant ES 03817 from the National Institutes of Environmental Health Sciences, NIH, to D.R.W. SSRL is funded by the Department of Energy, Offices of Basic Energy Sciences and Biological and Environmental Research, and the National Institutes of Health, National Center for Research Resources, Biomedical Technology Program. National Institutes of Health Grant 5P30-CA 42014 provided support to the Biotechnology Core Facility for DNA synthesis and to the DNA Sequencing Facility at the University of Utah for DNA sequencing.

* To whom correspondence should be addressed. Telephone: 801-585-5103. Telefax: 801-585-5469. Email: dennis.winge@hsc.utah.edu.

‡ University of Utah Health Sciences Center.

§ Stanford Synchrotron Radiation Laboratory.

10.1021/bi002315x CCC: $20.00
Published on Web 12/20/2000

homologous *SCO2* (*10*). Cox17 is proposed to shuttle Cu ions to the mitochondria and transfer Cu to Sco1 as an intermediate step in Cu metalation of cytochrome *c* oxidase (*10*). Cox11 is critical for Cu_B site formation in *Rhodobacter sphaeroides* (*12*). If yeast Cox11 is a metallochaperone for the Cu_B site of cytochrome oxidase, the possibility exists that CuCox17 delivers Cu(I) to both Sco1 and Cox11 for subsequent donation to the Cu_A and Cu_B sites, respectively.

Previously, we showed that yeast Cox17 bound two Cu(I) ions with thiolate ligation (*14*). Recombinant Cox17 expressed as a GST[1] fusion was found to bind two Cu(I) ions per molecule before and after cleavage of the GST moiety by thrombin. X-ray absorption spectroscopy of the CuCox17 complex revealed that the Cu(I) ions cluster in a polycopper thiolate center (*14*). The CuCox17 complex was pH-labile with Cu(I) ions dissociating near pH 5. The complex exhibited a brownish hue that was bleached by acidification. One sulfide ion was detected per Cox17 molecule in the Cu conformer.

Due to poor yields in the cleavage of the GST purification tag, we attempted to purify the untagged Cox17 in bacteria. We report presently the characterization of purified untagged CuCox17. Curiously, the physical properties differ from those of Cox17 purified as a GST-tagged protein. A discussion is presented of possible reasons for altered properties of Cox17 isolated with a GST tag. The untagged CuCox17 complex contains a polycopper thiolate cluster with similar properties to the clusters that form in the Cup1 metallothionein and Ace1 transcription factor. The functional CuCox17 complex is also oligomeric. The importance of oligomerization in function is discussed.

MATERIALS AND METHODS

Protein Purification. COX17 expression vectors were constructed using PCR. The 5′ oligonucleotide was constructed to include a 5′ *Nde*I site and the first five codons optimized for *E. coli* expression. The 3′ oligonucleotide was synthesized containing a 3′ *Bam*HI site. The PCR product was digested with *Nde*I/*Bam*HI and subcloned into a pET3 derivative, pAED4. *E. coli* strain BL21 (pLysS) was transformed with pAED3 vectors containing *cox17* variants using dimethyl sulfoxide competent cells. Transformants pregrown to an A_{600} of 0.4−0.6 absorbance unit were induced by the addition of 0.3 mM isopropyl thio-β-D-galactosidase and incubated an additional 3 h. $CuSO_4$ was added to a final concentration of 1.4 mM 1 h before harvest. Cells were washed thoroughly with 0.25 M sucrose to remove spuriously bound Cu(II). Cells were lysed by freeze−thawing and repeated sonication in lysis buffer: 20 mM phosphate, pH 7.0, 1 mM dithiothreitol (DTT). The lysate was clarified by centrifugation at 100000*g* for 40 min at 4 °C. All chromatography was performed utilizing an AKTA Fast Protein Liquid Chromatography unit (Amersham Pharmacia). The supernatant was filtered through a 0.45 μm filter and loaded onto a HiPrep 16/10 DEAE column equilibrated with lysis buffer. The protein was eluted in a 0−0.4 M KCl gradient. Fractions containing Cox17 were combined, diluted 2-fold, and loaded on the hydroxyapatite column equilibrated with lysis buffer. Protein was eluted in a 20−200 mM phosphate gradient (pH 7.0). Fractions containing Cox17 were concentrated and subjected to size exclusion chromatography on a G-75 Superdex 26/60 column equilibrated in 50 mM phosphate, pH 7.0, 1 mM DTT, and 100 mM NaCl. Analytical gel filtration was performed using a 10/30 G-75 Superdex size exclusion column equilibrated with 20 mM phosphate, pH 7, 100 mM NaCl, and 1 mM DTT. Data were recorded using Unicorn software.

Purified Cox17 was prepared for mass spectrometry by dialysis for 16 h in acetate buffer, pH 5, containing 1 mM DTT followed by dialysis in 5 mM Tris-HCl, pH 7, containing 1 mM DTT. Electrospray and matrix-assisted laser desorption ionization mass spectrometries were done at the Scripps Research Institute mass spectrometry facility.

Assays. The copper concentration of the protein samples was measured using a Perkin-Elmer (AAnalyst 100) atomic absorption spectrophotometer. Protein was quantified by amino acid analysis after hydrolysis in 5.7 N HCl at 110 °C in vacuo. A Beckman 6300 analyzer was used for the analyses. Sulfide was quantified as described previously (*17*). Ligand exchange was measured by BCS competition studies with Cox17. The appearance of a $Cu(BCS)_2$ complex was measured by monitoring the absorbance at 483 nm with respect to time using a molar extinction coefficient of 12 250 (*18*). All BCS titrations were performed in the absence of DTT.

Spectroscopy. Optical absorption spectroscopy was carried out on a Beckman DU640 of Cox17 samples dialyzed in 20 mM phosphate, pH 7, 100 mM NaCl. pH titrations were done in 20 mM phosphate, pH 7. The change in A_{254} was monitored with the addition of HCl. Measurements of pH were taken directly on samples for which the absorption was measured. Luminescence was measured on a Perkin-Elmer 650-10S fluorometer with the excitation set at 300 nm. Samples of Cup1, Ace1, and Cox17 were compared at a concentration of 28 μM.

X-ray absorption spectroscopy was carried out at the Stanford Synchrotron Radiation Laboratory with the SPEAR storage ring operating at 3.0 GeV and containing 60−100 mA. Copper K-edge data were collected on beamline 7-3 using a Si(220) double crystal monochromator, with an upstream vertical aperture of 1 mm, and a wiggler field of 1.8 T. Harmonic rejection was accomplished by detuning one monochromator crystal to approximately 50% off-peak, and no specular optics were present in the beamline. The incident X-ray intensity was monitored using a nitrogen-filled ionization chamber, and X-ray absorption was measured as the X-ray Cu Kα fluorescence excitation spectrum using an array of 13 germanium intrinsic detectors. During data collection, samples were maintained at a temperature of approximately 10 K, using an Oxford Instruments liquid helium flow cryostat. Ten 30 min scans were accumulated, and the absorption of a copper metal foil was measured simultaneously by transmittance. The energy was calibrated with reference to the lowest energy inflection point of the copper foil, which was assumed to be 8980.3 eV. EXAFS data analysis was done using the EXAFSPAK software (www-ssrl.slac.Stanford.edu/esafspak.html), and the phase and amplitude functions were calculated using the ab initio code Feff version 7.02 (*19*, *20*). Two synthetic copper model

[1] Abbreviations: EXAFS, extended X-ray absorption fine structure spectroscopy; BCS, bathocuproine sulfonate; GST, glutathione *S*-transferase.

compounds were used: a trigonal $[Cu_4(SPh)_6]^{2-}$ cluster (*21*) and a digonal $[Cu(SC_{10}H_{12})_2]^{2-}$ compound (*22*).

Sedimentation Equilibrium Ultracentrifugation. Sedimentation equilibrium experiments were used to gain insight into the solution states of Cox17. Experiments were conducted in a Beckman Optima XL-A analytical ultracentrifuge, with an ATi60 rotor at 20 °C, using 6 channel, 12 mm thick, charcoal−epon centerpieces. The three sample channels in each cell contained three different loading concentrations of protein, while reference channels contained the dialysate. Initial loading concentrations of protein, in 20 mM Tris, pH 7.0, + 100 mM NaCl, ranged from 2 to 30 μM. Samples were centrifuged at speeds ranging from 32 500 to 40 000 rpm until sedimentation and chemical equilibrium were attained. Cells were scanned radially in continuous mode, with data resulting from 10 absorbance readings taken at 0.001 cm intervals and 254 nm. Equilibrium was confirmed by no change in scans taken at 4 h intervals.

Large concentration gradients at the base of the cell can give rise to refractive index gradients that may result in anomalous light redirection. To avoid this problem, a baseline scan at a nonabsorbing wavelength (600 nm) was taken once equilibrium was attained. Significant deviations from zero absorbance occur as a result of light redirection, and thus these scans can be used to indicate the radial position above which the absorbance data become unreliable.

Various models describing the concentration distribution were fit to final absorbance versus radius data using nonlinear least-squares techniques and the analysis program NONLIN (*23*). NONLIN performs simultaneous nonlinear least-squares fits to one or more sets of ultracentrifuge data. This program was used to determine molecular weights, association constants, and virial coefficients. In each case, the final fit resulted from the simultaneous fitting of three different concentration distributions. To avoid the problem of relative local minima in the variance space, the fitting procedure was begun at many different initial points spanning the range of the parameters. A baseline-offset term was incorporated to account for the zero offset of the optical system or the presence of any absorbing, nonsedimenting components. A value of 0.73 mL/mg was used for the partial specific volume in each case.

Quantitation of Cellular Cox17 Levels. Cox17 levels were quantified in cells using western analysis with polyclonal antisera to Cox17 described previously (*15*). A standard curve was created by loading varying amounts of Cox17 purified protein on a 15% polyacrylamide gel. Proteins were blotted on nitrocellulose and probed for Cox17 using a 1:5000 dilution of the Cox17 antisera. Horseradish peroxidase conjugated anti-rabbit antibody was used as a secondary antibody at a 1:1000 dilution. Cox17 was visualized using ECL reagents (Amersham Pharmacia Biotech). The amount of cellular Cox17 was determined by comparison with the lanes containing known amounts of purified Cox17 to the lanes containing whole cells. The yeast cell volume was taken to be 1×10^{-14} L per cell. Previously, it was reported that 60% of the cellular Cox17 was found within the IM space of mitochondria (*13*). The mitochondrial content of yeast cultured in glucose medium is estimated to represent 3% of the cell volume (*24*).

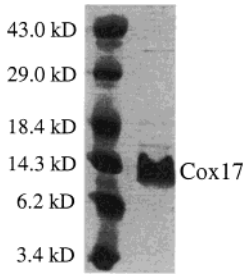

FIGURE 1: Purified Cox17 as shown by Coomassie stain on an SDS−polyacrylamide gel. Protein without an affinity tag was produced in *E. coli*. Purification to greater than 95% was accomplished by conventional chromatography.

RESULTS

Expression of untagged *COX17* in *E. coli* on an IPTG-inducible plasmid resulted in accumulation of soluble CuCox17 in the cell lysate. CuCox17 was purified by a combination of anion exchange chromatography, hydroxyapatite chromatography, and gel filtration. The yield of pure Cox17 was over 3 mg per liter of culture. The purified protein showed a single component on SDS−polyacrylamide gel electrophoresis (Figure 1), and showed the expected amino acid composition after acid hydrolysis. Mass spectroscopy of the purified sample gave two components with masses of 7926 and 8056 Da. The predicted mass of the intact protein was 8056.05 Da. The second component was 130 Da lighter, consistent with a fraction of desMet polypeptides. This was confirmed by Edman sequence analysis showing that the purified sample contained nearly equal quantities of protein with the N-terminal Met intact and the desMet polypeptide.

The protein as isolated contained 3 ± 0.5 ($n = 8$) mol equiv of Cu per polypeptide. Extensive dialysis of the CuCox17 sample in buffer containing 1 mM DTT did not alter the bound Cu content. Electrospray mass spectrometry failed to show any significant metalated species even with varying the skimmer potential. The major species observed were the two apo-species. The CuCox17 complex exhibited only a slight amber hue at 10 mg/mL. This is in contrast to the blackish hue of the CuCox17 complex purified as a GST fusion. The untagged CuCox17 showed no significant levels of labile sulfur (0.03 mol equiv), whereas the GST-Cox17 fusion contained 0.9 mol equiv of acid-labile sulfide.

The purified, untagged CuCox17 protein exhibits transitions in the ultraviolet region that are bleached upon acidification consistent with thiolate−Cu charge-transfer transitions (Figure 2A). A hydrogen ion concentration corresponding to pH 1 is needed to bleach the transitions (Figure 2A, inset). The Cu(I) complex of the *CUP1* metallothionein that forms a heptacopper thiolate cluster exhibits similar acid-labile, thiolate−Cu charge-transfer transitions in the ultraviolet. A higher hydrogen ion concentration is necessary to bleach the transitions in the CuCup1 complex (Figure 2A, inset). In contrast, the Cu(I) complex of GST−Cox17 was labile at pH 5. The S−Cu charge-transfer bands of the GST−Cox17 Cu complex were bleached below pH 5 (*14*).

The CuCox17 complex is luminescent with an emission maximum near 570 nm (Figure 2B). This emission is diagnostic of multinuclear Cu(I) complexes in solvent-shielded environments. The relative quantum yield is intermediate between the emission yield of the heptacopper

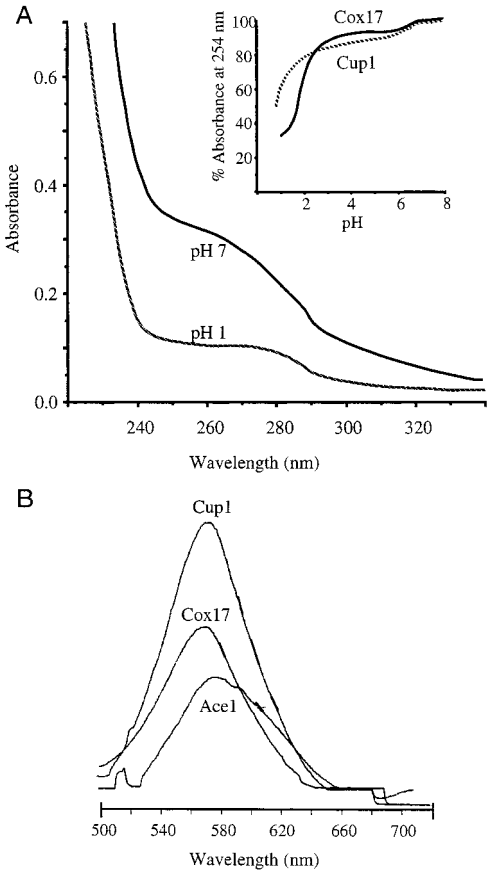

FIGURE 2: Panel A: UV absorption spectrum of Cox17. The protein, at pH 7, exhibits a broad absorbance from 250 to 270 nm (solid line). This absorption is bleached by addition of acid to pH 1 (dotted line). The inset shows an acid stability comparison between the Cu(I) thiolate centers of Cox17 and Cup1 by measuring the decrease in absorption at 254 nm verses pH. Panel B: Cu(I) luminescence of CuCox17 compared to CuCup1 and CuAce1. The excitation wavelength was 300 nm, and the emission was monitored from 500 to 670 nm with the emission maxima being at 570 nm. The copper concentration of each sample was equivalent.

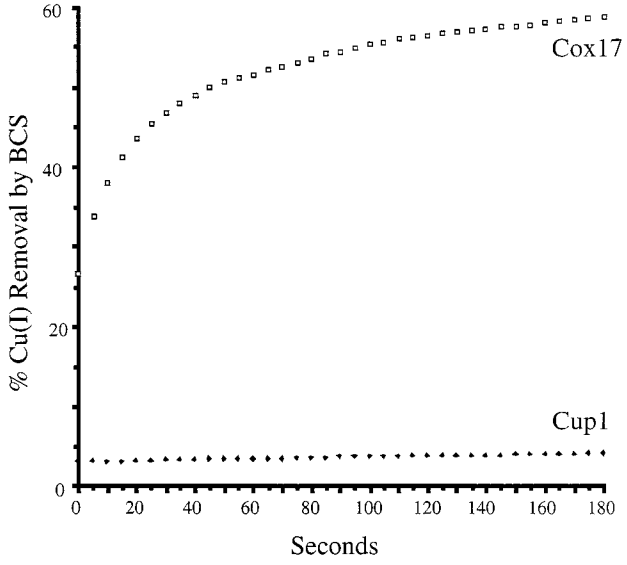

FIGURE 3: Ligand exchange reaction of CuCox17 and CuCup1 with the Cu(I) chelator bathocuproine sulfonate (BCS). The formation of the $Cu(BCS)_2$ complex was monitored at 483 nm. Fifty percent of the Cu(I) in Cox17 reacts with BCS within 30 s.

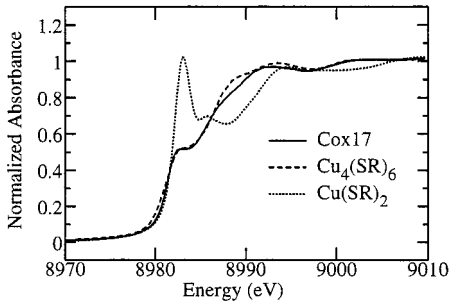

FIGURE 4: X-ray absorption near-edge spectra of CuCox17 and two model Cu(I) thiolate compounds. A trigonal Cu(I) complex, $[Cu_4(SPh)_6]^{2-}$ (*21*), and a digonal Cu(I) complex, $[Cu(SC_{10}H_{12})_2]^{2-}$ (*22*), were used.

thiolate cluster in CuCup1 and the tetracopper thiolate cluster in CuAce1 at equivalent copper ion concentrations. The relative quantum yields of CuCox17 and CuCup1 show a linear dependency with Cu ion concentrations over a 10-fold concentration range. The combination of the ultraviolet absorption and emission data is suggestive that untagged CuCox17 contains a solvent-shielded polycopper center. To test how reactive the Cu(I) ions are in Cox17 to exogenous ligands, the CuCox17 complex was incubated with the Cu(I) chelator bathocuproine disulfonate (BCS) (Figure 3). A subset of the Cu(I) ions in Cox17 equilibrated rapidly with BCS, whereas the remaining Cu(I) ions exhibited slow kinetics of reactivity with BCS. The Cu(I) ions in the buried heptacopper cluster in CuCup1 showed limited reactivity with BCS.

X-ray absorption spectroscopy confirmed that untagged CuCox17 contained a polynuclear Cu(I) cluster. The copper K edge showed a feature at 8983 eV consistent with a 1s→ 4p transition of Cu(I) ions (*25*) (Figure 4). The energy and intensity of the near-edge feature are similar to those seen in the trigonal $[Cu_4(SPh)_6]^{2-}$ Cu(I) thiolate cluster but unlike edge features of the digonal $[Cu(SC_{10}H_{12})_2]^{2-}$ Cu(I) thiolate compound (*25*, *26*). The intensity of the edge peak of digonally coordinated Cu(I), unlike the edge feature in CuCox17, approaches that of the absorption continuum (*25*, *26*).

Fourier transform analysis of the Cu K-edge EXAFS revealed two prominent shells of interactions with absorbing Cu(I) ions (Figure 5, top line of bottom panel). The first transform peak at 2.25 Å arises from the first shell ligand backscattering. The EXAFS generating the first shell peak was best fit with three sulfur ligands at 2.25 Å (Table 1). Fits of the EXAFS assuming nitrogen or oxygen ligands were inferior. This distance is consistent with trigonal Cu(I) coordination (*27*). The second transform peak at about 2.7 Å was best fit with the inclusion of a heavy Cu scatterer atom. This peak confirms the existence of a polycopper cluster in Cox17. The CuCox17 complex purified as a GST fusion also showed a similar Cu−Cu backscatter peak at 2.7 Å; however, the magnitude of the Cu−Cu scatter peak is much less prominent than that in the untagged CuCox17 complex. Outer shell Cu−Cu interactions at 2.7−2.74 Å are seen in the polycopper thiolate clusters in CuCup1 and CuAce1 (*27*). A comparison of the EXAFS Fourier transforms of CuCox17, CuCup1, and CuAce1 is shown in Figure 6. The magnitude of the Cu−Cu scatter peak is most prominent for the CuCox17 complex.

Previously, we demonstrated that three of the seven cysteinyl residues in yeast Cox17 are critical for function

Table 1: Cu K-Edge EXAFS Curve-Fitting Results[a]

	Cu−S			Cu−Cu			
	N	*R* (Å)	σ^2 (Å^2)	*N*	*R* (Å)	σ^2 (Å^2)	*F*
wild-type	3.0 (1)	2.250 (2)	0.0045 (2)	1.2 (1)	2.705 (2)	0.0052 (6)	0.221
C23S	2.9 (1)	2.245 (2)	0.0044 (2)	1.1 (1)	2.706 (3)	0.0065 (7)	0.189
C24S	2.6 (1)	2.253 (3)	0.0036 (3)	1.2 (3)	2.698 (5)	0.0078 (1)	0.309
C26S	2.6 (1)	2.242 (2)	0.0054 (3)	1.2 (3)	2.708 (5)	0.0108 (16)	0.261
C16,36,47S	2.8 (1)	2.252 (2)	0.0038 (2)	1.8 (1)	2.716 (2)	0.0059 (4)	0.175

[a] *N* is the coordination number, *R* is the mean interatomic distance, σ^2 is the mean square deviation in *R*, and *F* is the fit error function. The fit error is defined as $[\Sigma(\chi_{expt} - \chi_{calc})^2k^6/\Sigma\chi_{calc}{}^2k^6(\sigma_{calc}{}^2k^6)]^{1/2}$, and the results given are those in which the coordination numbers and Debye−Waller factors were simultaneously refined. The values given in parentheses are estimated standard deviations (precisions) obtained from the diagonal elements of the covariance matrix. We note that the accuracies will be larger than these values, and can be assumed to be ±0.02 Å, and ±0.2 for Cu−S and ±0.5 for Cu−Cu coordination numbers.

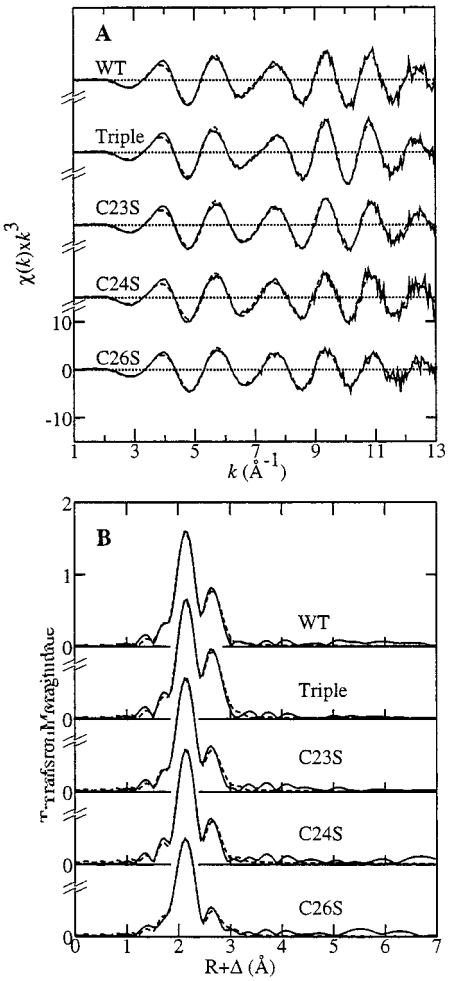

FIGURE 5: EXAFS of wild-type untagged CuCox17 and various mutant forms (panel A) and corresponding Fourier transforms (phase-corrected for Cu−S backscattering) (panel B). In both panels A and B, the solid lines are the experimental data, and the broken lines are the best fit. The parameters from the fits are shown in Table 1. The wild-type and triple mutant were analyzed at a final Cox17 Cu concentration of 2 mM. The $C_{23}S$, $C_{24}S$, and $C_{26}S$ mutant proteins were analyzed at 4 mM Cu. The protein samples were in 50 mM phosphate, pH 7, with 100 mM NaCl.

(*15*). The three critical cysteinyl residues are part of a CysCysXaaCys sequence motif. Single Cys→Ser substitutions at the three critical Cys residues (Cys23, Cys24, and Cys26) or any of the four nonessential Cys residues (Cys16, Cys36, Cys47, and Cys57) do not alter the ability of the protein to bind three Cu(I) ions (*15*). Cox17 molecules with a double $Cys_{23,24}$Ser substitution fail to bind Cu(I). In contrast, multiple Cys→Ser substitutions at nonessential Cys

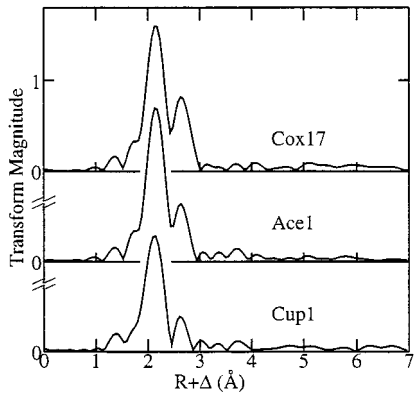

FIGURE 6: EXAFS Fourier transforms of CuCox17, CuAce1, and CuCup1. The Cu regulatory domain of Ace1 consisting of residues 35−110 was used. This domain binds four Cu(I) ions per monomer. The Cup1 metallothionein binds seven Cu(I) ions in a single heptacopper thiolate cluster (*33*). In all cases, the Fourier transforms are phase-corrected for Cu−S backscattering.

residues do not impair Cu(I) binding. A triple mutant containing a $Cys_{16,36,47}$Ser substitution is functional and binds three Cu(I) ions (*15*). The EXAFS of the triple $C_{16,36,47}S$ Cox17 mutant were similar to those of the wild-type Cox17 in that both show intense backscattering from three Cu−S ligands at 2.25 Å. However, the Cu−Cu interactions are significantly different. For the triple mutant, the EXAFS curve-fitting analysis suggests a Cu−Cu coordination number of about 1.8 (Table 1), whereas for the wild-type this value is closer to 1.2 (Figure 5, Table 1). The combination of the observed stoichiometry of 3 mol equiv of Cu(I) and short 2.7 Å Cu−Cu distance in the EXAFS of wild-type and the functional $Cys_{16,36,47}$Ser triple mutant is consistent with both proteins containing a polycopper cluster. Although cysteine residues, C16, C36, and C47, are not essential for activity, they appear to subtly influence the structure of the polycopper cluster. At first sight, this might seem surprising; it is not without precidence as long-distance interactions are known to modify the physical properties of other metalloprotein metal centers, e.g., Fe_4S_4 cluster electrochemistry and Zn(II) site electrostatics (*28*).

Single Cys→Ser substitutions at the three critical Cys residues (Cys23, Cys24, and Cys26) do not abrogate Cu(I) binding. The EXAFS of the Cys_{23}Ser, Cys_{24}Ser, and Cys_{26}Ser mutants show clear Cu−Cu backscattering consistent with the presence of a polycopper center in each. In contrast to the triple mutant, the magnitude of the outer shell Cu−Cu peak in the Fourier transform is less than that of the wild-type protein (Figure 5). The reduced Cu−Cu transform peak

amplitude arises from an increased Debye−Waller factor (relative to the wild-type protein), suggesting an increase in the distribution of Cu−Cu distances in the polycopper cluster. We also note that it is possible that non-native types of polycopper clusters may form in these mutants with one or more of the four nonessential cysteines serving as ligands.

To determine whether the Cu complex was contained within a monomeric or oligomeric protein, we carried out analytical gel filtration on Sephadex G-75 of purified protein. The elution profile of Cox17 revealed at least three components eluting in volumes equivalent to higher molecular mass species (Figure 7A). The ratio of the three components varied depending on the Cox17 protein concentration (Figure 7A). The higher the initial Cox17 concentration, the more predominant was the high molecular mass species (Figure 7B). Each component revealed the same Cox17 polypeptide by SDS−polyacrylamide gel electrophoresis and amino acid analysis (data not shown). The Cu binding stoichiometry was equivalent for the three components. The concentration-dependent oligomeric nature of Cox17 was reversible. Concentration of the purified lowest molecular mass component followed by rechromatography resulted in the conversion of the lower molecular mass component to a mixture of the two higher molecular mass species (data not shown).

Mutant Cox17 molecules with Cys→Ser substitutions were evaluated for oligomerization. Mutant Cox17 molecules purified to homogeneity were evaluated by analytical gel filtration. A functional, triple mutant with $Cys_{16,36,47}Ser$ substitutions (nonessential cysteines) exhibited the same oligomerization pattern as the wild-type protein (data not shown). In contrast, Cox17 molecules with single Cys→Ser substitutions at the essential Cys positions 23, 24, or 26 did not show the high molecular mass species observed with the wild-type protein (Figure 7B). The mutant protein with a double $Cys_{23,24}Ser$ substitution that fails to bind Cu(I) eluted predominantly as the lowest molecular mass species (Figure 7B).

Sedimentation equilibrium was carried out to determine the oligomeric species present in the wild-type and mutant proteins. Models describing the association behavior of Cox17 were simultaneously fit to up to three different concentration distributions resulting from various speeds and loading concentrations. The best fit of the wild-type CuCox17 data over the concentration range examined was obtained with an equilibrium between predominantly dimers and tetramers, with the dimeric mass set at 16 110 Da (Figure 8A). The fit to a two-species equilibrium resulted in small and randomly distributed residuals about zero. The equilibrium constant derived for this equilibrium corresponded to a dissociation constant of 20 ± 10 μM. The fit to a monomer/dimer equilibrium did not yield an acceptable fit. In contrast, equilibrium centrifugation of the $Cys_{23}Ser$ or $Cys_{24}Ser$ mutant Cox17 was best fit as predominantly a monomer/dimer equilibrium, consistent with the gel filtration behavior of the mutant proteins (Figure 8B). The $Cys_{23}Ser$ Cox17 mutant behaved identically to the $Cys_{24}Ser$ mutant protein. The residuals of the fit were randomly distributed around zero, indicating a good fit. The dissociation constant of the monomer/dimer equilibrium was best fit as 1.3 ± 1 μM. Sedimentation analysis of the non-copper binding $Cys_{23,24}$-Ser mutant Cox17 protein showed a monomer/dimer equilibrium, but the equilibrium was shifted toward the monomer relative to the single mutant Cox17 molecules.

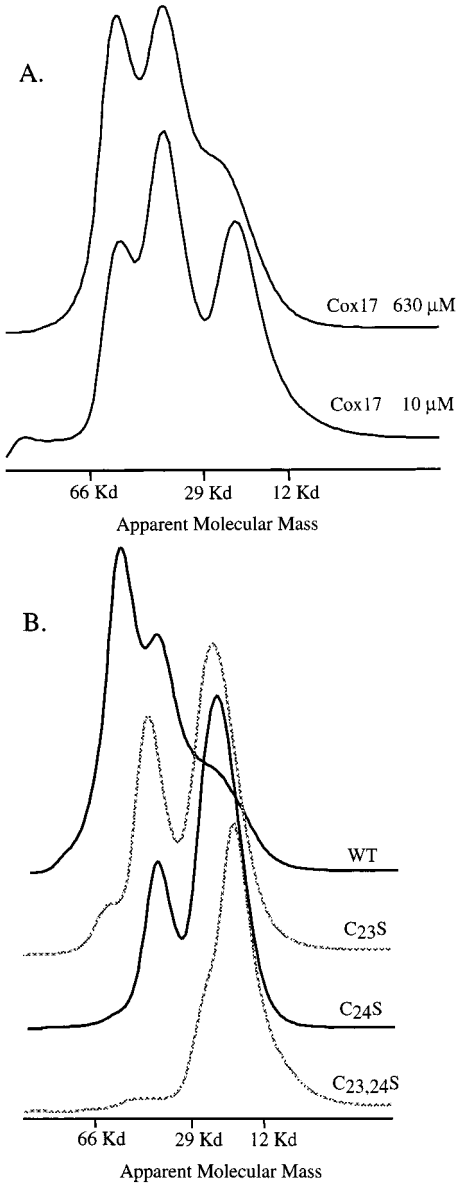

FIGURE 7: Gel filtration of Cox17. The protein was analyzed on a G-75 analytical Superdex column. Panel A: Gel filtration of wild-type CuCox17 showing three separate Cox17 species. The starting Cox17 protein concentrations were 630 μM for the top chromatogram and 10 μM for the bottom chromatogram. Each of these peaks was composed exclusively of Cox17. The peaks eluted at apparent molecular masses of 16, 38, and 53 kDa. Reconcentration of the 10 μM sample to a final concentration of 630 μM resulted in a shift to predominantly higher molecular mass species. Panel B: Gel filtration comparing wild-type Cox17 with nonfunctional Cox17 mutants. At 630 μM Cox17, the wild-type protein aggregated to primarily the highest order oligomeric species. $C_{23}S$, $C_{24}S$, and $C_{23,24}S$ mutant Cox17 molecules lacked the higher order oligomeric species.

The dimeric (16 110 amu) and tetrameric (32 220 amu) Cox17 samples elute on gel filtration with apparent molecular masses of 38 000 and 55 000 Da. The higher apparent molecular mass of the Cox17 oligomers by gel filtration is consistent with CuCox17 being elongated in structure, since elution from gel filtration correlates with the Stokes radius of a molecule.

The cellular Cox17 protein levels were quantified by western analysis to compare to the concentration-dependent oligomerization equilibrium measured in vitro. Serial dilu-

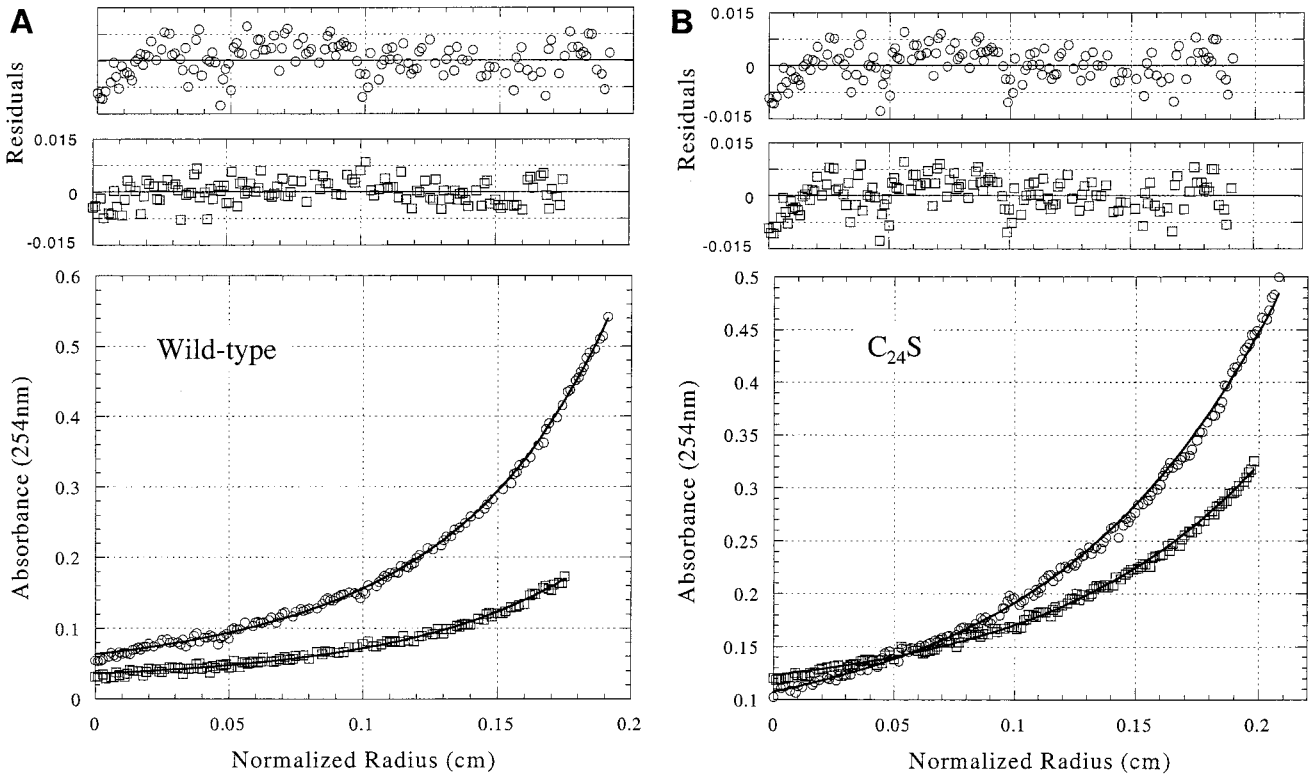

FIGURE 8: Equilibrium sedimentation analysis of the wild-type Cox17. Panel A: The lower box shows the data points for two different concentrations of Cox17 (28 and 7 μM). The solid line through these points represents the fit to a two-species equilibrium with the lowest species set to the Cox17 dimer molecular mass of 16 110 daltons. The fit represents a dimer/tetramer equilibrium. The k_d for the equilibrium is 20 $\pm$ 10 μM. The upper two panels show the residuals for the fit of each of the two Cox17 concentrations with the 28 μM sample on top. Panel B: Equilibrium sedimentation analysis of the Cys_{24}Ser Cox17. The lower box shows the data points for two different concentrations of Cox17. The solid line through these points represents the fit to a two-species equilibrium with the lowest species set to the Cox17 monomer molecular mass of 8055 daltons. The fit represents a monomer/dimer equilibrium. The k_d for the equilibrium is 1.3 $\pm$ 1 μM. The upper panels show the residuals for the fit of each of the Cox17 concentrations. The upper panel shows the residuals from the fit for the more concentrated Cox17 sample. The middle panel shows the residuals from the fit for the less concentrated sample.

tions of purified Cox17 were electrophoresed on an acrylamide gel and visualized by western analysis using Cox17 polyclonal antisera. The total cellular content of Cox17 was found to be 5×10^{-7} ng. Previously, it was reported that 60% of Cox17 was localized to the intermembrane space and 40% was in the cytoplasm (*13*). Using a cell volume of 7×10^{-14} L (*29*), the cytoplasmic concentration of Cox17 is approximately 0.4 μM. Since the volume of yeast mitochondria is approximately 3% of the cell volume in exponentially growing cells, and the IM space is 10% of the mitochondrial volume, the Cox17 concentration in the IM space is greater than 60 μM. Thus, it is likely that Cox17 forms dimers and tetramers within the mitochondria.

DISCUSSION

The CuCox17 complex purified as an untagged molecule is an asymmetric, oligomeric complex with one or more polycopper clusters. The polycopper cluster(s) in Cox17 exhibit(s) many features of the copper thiolate clusters that form in the Cup1 metallothionein and the Ace1 transcription factor. Each molecule forms a cluster with predominantly trigonal Cu(I) coordination by cysteinyl thiolates. The clusters are pH-stable and luminescent consistent with solvent shielding. The CuCox17 complex is distinct from the CuCup1 and CuAce1 clusters in its lability to ligand exchange reactions using the Cu(I) chelator bathocuproine sulfonate.

The biophysical properties of the polycopper cluster in untagged Cox17 are distinct from the properties of Cox17 purified previously as a GST fusion protein (*14*). The cluster that forms in GST−Cox17 is labile at pH 5, weakly emissive, and contains a single labile sulfur atom. The blackish coloration of the complex is consistent with the presence of a labile sulfur atom. The unusual polycopper cluster that forms in GST−Cox17 persists even after the GST purification tag is proteolytically removed. It is likely that an artifactual CuS cluster forms in GST−Cox17 due to the obligate dimeric state of GST. The dimerization of GST must result in a non-native conformer in Cox17 induced by Cu(I) binding and that persists even after cleavage of the GST tag. If Cu−thiolate coordinate bonding is a major driving force for the polypeptide folding of Cox17 as in Cup1 and Ace1 (*30*), the dimeric GST fusion may result in a kinetically trapped non-native CuS cluster in Cox17.

The Cu(I) complexes of both the untagged Cox17 and the GST−Cox17 molecules are polynuclear. The cleaved GST−Cox17 complex consisted of two bound Cu(I) ions in contrast to the stoichiometry of 3 mol equiv for the untagged Cox17 molecule. EXAFS of both the cleaved GST−Cox17 sample and the untagged CuCox17 molecule exhibited clear outer shell photoelectron scatter peaks at 2.7 Å consistent with a polycopper cluster. The magnitude of the Cu−Cu scatter peak is significantly greater for the untagged CuCox17 than the GST−Cox17 complex. The increased magnitude suggests

that the polycopper cluster in the untagged Cox17 is more uniform than that observed in the GST−Cox17 fusion.

The untagged CuCox17 complex is a mixture of oligomeric species with the major components being dimers and tetramers. The species interconvert in a concentration-dependent manner. The dimer/tetramer equilibrium does not alter the observed Cu binding stoichiometry of 3 mol equiv and appears to not alter the luminescence of the complex. The relative quantum yield of luminescence was linear over a 10-fold concentration range, a range in which the dimer/tetramer ratio changes appreciably. Low levels of monomeric CuCox17 exist at low protein concentrations, but the major species are the dimeric and tetrameric molecules.

The nuclearity of the polycopper cluster in untagged Cox17 is not obvious. The dimeric species should contain six Cu(I) ions. Two models for the CuS center exist. First, the dimeric species may contain two separate trinuclear Cu centers. A trinuclear Cu cluster is expected to have at least four ligands if each Cu(I) ion exhibits trigonal coordination. Second, the six Cu(I) ions may exist within a single hexacopper center. Small synthetic hexacopper cage clusters are known (*31*). The known hexacopper clusters contain either all trigonally bound Cu(I) ions or a mixture of trigonally and digonally coordinated Cu(I) ions (*31*). The minimal number of ligands for a trigonally coordinated hexacopper cluster is 8. If a hexacopper cluster exists at the dimer interface, the presence of low quantities of monomeric CuCox17 species would necessitate a different center in the monomer. The monomer appears to be in equilibrium with the higher order oligomers, so it is unlikely that major rearrangements occur within the Cu center. The most definitive demonstration of limited quantities of monomeric species was from gel filtration studies which were done in a buffer with DTT thiolates, so the possibility exists that DTT may provide a thiolate ligand in the monomer.

We demonstrated that only three thiolates in Cox17 are essential for in vivo function (*15*). These cysteines are part of a conserved CysCysXaaCys sequence motif. These three thiolates are candidate ligands for the polycopper cluster. A mutant form of Cox17 with the CysCys sequence altered to SerSer fails to bind Cu(I). Assuming these three thiolates are involved in Cu(I) ligation, at least one additional ligand is expected for a trinuclear Cu(I) center in a monomer. The best fit of the EXAFS of wild-type untagged Cox17 suggests all-thiolate ligation. A trinuclear Cu(I) center in a monomer could form with three μ doubly bridging sulfurs and one μ_3 triply bridging sulfur. If the polycopper cluster formed at the dimer interface, a hexacopper cluster could form with four ligands from each monomer yielding a Cu_6S_8 center. The identity of the fourth sulfur ligand is unclear. The fourth ligand must come from one of the remaining Cys residues or the conserved Met58. Although Cox17 molecules with single Cys→Ser substitutions at positions16, 36, 47, or 57 or a Met_{58}Ser substitution are functional, quadruple mutants with $Cys_{16,36,47,57}$Ser or $Cys_{16,36,47}$Ser, Met_{58}Ser substitutions are nonfunctional in vivo. Cys36, Cys47, Cys57, and Met58 are highly conserved residues in Cox17 molecules from various species, so it is conceivable that all of these sulfur atoms project toward the Cu(I) cluster and different combinations of sulfurs may be used to form the polycopper cluster. Molecules lacking Cys36 and Cys47 may use one or both sulfur ligands from Cys57 or Met58. Molecules lacking Cys57 or Met58 may use one or both sulfur ligands from Cys36 or Cys47. The current spectroscopic data on wild-type Cox17 and the mutant forms are of insufficient information content to resolve the type of polycopper center.

Cox17 mutants with Cys→Ser substitutions in any one of the essential Cys residues (C23, C24, or C26) are nonfunctional, but their Cu(I) binding stoichiometry is unchanged, despite losing a candidate ligand. Although these mutants bind normal quantities of Cu(I) in polycopper clusters, the observed outer shell scattering attributed to the short Cu−Cu distance in the wild-type protein is significantly reduced for each mutant. Non-native types of polycopper clusters likely form in these mutants. It is conceivable that structural rearrangements occur in these mutants enabling one or more of the four nonessential cysteines to serve as ligands. Structural rearrangements to accommodate a non-native ligand are known in *Azotobacter* ferredoxin (*32*).

The reactivity of CuCox17 with bathocuproine sulfonate revealed that only two of the three Cu(I) ions were in rapid exchange with the chelator. This may arise from one of three scenarios. First, incomplete BCS reactivity of CuCox17 may arise from different ligand exchange kinetics of two distinct polycopper centers within the dimer. Second, ligand exchange reactions may differ between the dimer and tetramer species. Third, the Cu(I) ions within a single polymetallic cluster may exhibit differential solvent accessibility. The present data do not distinguish between the models.

The oligomeric state of Cox17 changes in mutant forms of the proteins involving any one of the essential cysteines. The C_{23}S or C_{24}S Cox17 mutant does not aggregate to the tetrameric state. Rather, the molecules exhibit a monomer/dimer equilibrium, unlike the dimer/tetramer equilibrium of the wild-type protein. Furthermore, the non-Cu binding $C_{23,24}$S double mutant exists predominantly as a monomeric species. The nonfunctionality of the C_{23}S, C_{24}S, and C_{26}S Cox17 single mutants may arise from an altered conformation of the proteins or, alternatively, from an inability to oligomerize to a tetrameric species.

The oligomerization of Cox17 is concentration-dependent. The dissociation constant for the tetramer/dimer equilibrium is 20 μM. In the range of concentrations tested (0.02−600 μM), the protein was a mixture of predominantly dimers and tetramers. Only limited quantities of monomeric Cox17 species were observed. The concentration of Cox17 in the IM space exceeds 20 μM, so it is likely that an appreciable fraction of Cox17 exists in that space as a tetrameric complex.

Cox17 exhibits two novel features, namely, the polycopper cluster and oligomerization. Although the significance of these features is unclear, two distinct possibilities exist. First, the function of Cox17 as a Cu shuttle to the mitochondria predicts that CuCox17 ferries Cu(I) ions across the outer membrane. The outer membrane translocation may necessitate stabilizing Cu(I) ions within a polycopper cluster or within a oligomeric complex. Second, an oligomeric state of CuCox17 may be important in Cu(I) ion delivery to the Cu_A site assembly complex. The Cu_A site of cytochrome *c* oxidase (CcO) resides in a soluble domain of subunit II protruding into the inner membrane space of the mitochondrion. Cu_A site formation likely involves Sco1, and if Cu insertion into Cu_A takes place in the assembled CcO complex may involve the dimeric CcO complex. Bovine CcO exists

as a dimer with the two Cu_A centers separated by 74 Å (*2*). The dimer interface of bovine CcO within the IM space is formed by subunit VIb which also forms a tight interaction with CcO subunit II (*2*). The N-terminal residues of subunit VIb molecules are only separated by 26 Å. The corresponding subunit in yeast is Cox12. We have preliminary data that Sco1 forms a stable complex with CcO (Nittis and Winge, unpublished observation). It is unclear whether Sco1 docks onto Cox2 or Cox12 at the dimer interface. Thus, the possibility exists that Cox17 forms a transient complex with two Sco1 molecules docked onto either Cox2 or Cox12 within the IM space. The dimeric CuCox17 may be important for the Cox17/Sco1 interaction. Future studies will address these interactions.

ACKNOWLEDGMENT

Special acknowledgment is given Dr. Lisa Joss for assistance in sedimentation equilibrium analysis. We thank Dr. J. E. Penner-Hahn for giving us access to the XAS spectrum of the digonal $[Cu(SC_{10}H_{12})_2]^{2-}$ compound.

REFERENCES

1. Poyton, R. O., Goehring, B., Droste, M., Sevarion, K. A., Allen, L. A., and Zhao, X. J. (1995) *Methods Enzymol. 260*, 97−116.
2. Tsukihara, T., Aoyama, H., Yamashita, E., Tomizaki, T., Yamaguchi, H., Shinzawa-Itoh, K., Hakashima, R., Yaono, R., and Yoshikawa, S. (1995) *Science 269*, 1069−1074.
3. Poyton, R. O., and McEwen, J. E. (1996) *Annu. Rev. Biochem. 65*, 563−607.
4. Tzagoloff, A., Capitanio, N., Nobrega, M. P., and Gatti, D. (1990) *EMBO J. 9*, 2759−2764.
5. Glerum, D. M., and Tzagoloff, A. (1994) *Proc. Natl. Acad. Sci. U.S.A. 91*, 8452−8456.
6. Glerum, D. M., Koerner, T. J., and Tzagoloff, A. (1995) *J. Biol. Chem. 270*, 15585−15590.
7. Glerum, D. M., Muroff, I., Jin, C., and Tzagoloff, A. (1997) *J. Biol. Chem. 272*, 19088−19094.
8. Svensson, B., Andersson, K. K., and Hederstedt, L. (1996) *Eur. J. Biochem. 238*, 287−295.
9. Glerum, D. M., Shtanko, A., and Tzagoloff, A. (1996) *J. Biol. Chem. 271*, 14504−14509.
10. Glerum, D. M., Shtanko, A., and Tzagoloff, A. (1996) *J. Biol. Chem. 271*, 20531−20535.
11. Rentzsch, N., Krummeck-WeiB, G., Hofer, A., Bartuschka, A., Ostermann, K., and Rodel, G. (1999) *Curr. Genet. 35*, 103−108.
12. Hiser, L., Di Valentin, M., Hamer, A. G., and Hosler, J. P. (2000) *J. Biol. Chem. 275*, 619−623.
13. Beers, J., Glerum, D. M., and Tzagoloff, A. (1997) *J. Biol. Chem. 272*, 33191−33196.
14. Srinivasan, C., Posewitz, M. C., George, G. N., and Winge, D. R. (1998) *Biochemistry 37*, 7572−7577.
15. Heaton, D., Nittis, T., Srinivasan, C., and Winge, D. R. (2000) *J. Biol. Chem.* (in press).
16. Buchwald, P., Krummeck, G., and Rodel, G. (1991) *Mol. Gen. Genet. 229*, 413−420.
17. King, T. E., and Morris, R. O. (1957) *Methods Enzymol. 10*, 634−641.
18. Rifkind, J. M., Lauer, L. D., Chiang, S. C., and Li, N. C. (1976) *Biochemistry 15*, 5337−5343.
19. Rehr, J. J., Mustre de Leon, J., Zabinsky, S. I., and Albers, R. C. (1991) *J. Am. Chem. Soc. 113*, 5135−5140.
20. Mustre de Leon, J., Rehr, J. J., Zabinsky, S. I., and Albers, R. C. (1991) *Phys. Rev. 44*, 4146−4156.
21. Dance, I. G., Bowmaker, G. A., Clark, G. R., and Seadon, J. K. (1983) *Polyhedron 2*, 1031−1043.
22. Koch, S. A., Fikar, R., Millar, M., and O'Sullivan, T. (1984) *Inorg. Chem. 23*, 121−122.
23. Johnson, M. L., Correia, J. J., Yphantis, D. A., and Halvorson, H. R. (1981) *Biophys. J. 36*, 5775−5788.
24. Stevens, B. (1981) *The Molecular Biology of the Yeast Saccharomyces: Life Cycle and Inheritance* (Strathen, J. N., Jones, E. W., and Broach, J. R., Eds.) Cold Spring Harbor Laboratory Press, Cold Spring Harbor, NY.
25. Kau, L.-S., Spira-Solomon, D. J., Penner-Hahn, J. E., Hodgson, K. O., and Solomon, E. I. (1987) *J. Am. Chem. Soc. 109*, 6433−6442
26. Pufahl, R. A., Singer, C. P., Peariso, K. L., Lin, S.-J., Schmidt, P., Fahrni, C., Culotta, V. C., Penner-Hahn, J. E., and O'Halloran, T. V. O. (1997) *Science 278*, 853−856.
27. Pickering, I. J., George, G. N., Dameron, C. T., Kurz, B., Winge, D. R., and Dance, I. G. (1993) *J. Am. Chem. Soc. 115*, 9498−9505.
28. McCall, K. A., Huang, C.-C., and Fierke, C. A. (2000) *J. Nutr. 130*, 1437S−1446S.
29. Sherman, F. (1991) *Getting started with yeast*. in *Methods in Enzymology* (Gutherie, C., and Fink, G. R., Eds.) p 194, Academic Press, San Diego.
30. Winge, D. R., Dameron, C. T., and George, G. N. (1994) *Adv. Inorg. Biochem. 10*, 1−48.
31. Dance, I. G. (1986) *Polyhedron 5*, 1037−1104.
32. Shen, B., Jollie, D. R., Diller, T. C., Stout, C. D., Stephens, P. J., and Burgess, B. K. (1995) *Proc. Natl. Acad. Sci. U.S.A. 92*, 10064−10068.
33. Peterson, C. W., Narula, S. S., and Armitage, I. M. (1996) *FEBS Lett. 379*, 85−93.

BI002315X